Acta Cryst E CRYSTALLOGRAPHIC COMMUNICATIONS

ISSN 2056-9890

Received 15 March 2024
Accepted 2 May 2024

Edited by M. Weil, Vienna University of Technology, Austria

This article is part of a collection of articles to commemorate the founding of the African Crystallographic Association and the 75th anniversary of the IUCr.

Keywords: benzimidazol-2-one; crystal structure; triazole; C—H···π(ring) interaction; hydrogen bond.

CCDC reference: 2352892

Supporting information: this article has supporting information at journals.iucr.org/e

Crystal structure, Hirshfeld surface analysis, calculations of intermolecular interaction energies and energy frameworks and the DFT-optimized molecular structure of 1-[(1-butyl-1*H*-1,2,3-triazol-4-yl)methyl]-3-(prop-1-en-2-yl)-1*H*-benzimidazol-2-one

Zakaria El Atrassi,[a] Mustapha Zouhair,[a]* Olivier Blacque,[b] Tuncer Hökelek,[c] Amal Haoudi,[d] Ahmed Mazzah,[e] Hassan Cherkaoui[a] and Nada Kheira Sebbar[f,g]

[a]Laboratory of Heterocyclic Organic Chemistry, Medicines Science Research Center, Pharmacochemistry Competence Center, Mohammed V University in Rabat, Faculté des Sciences, Av. Ibn Battouta, BP 1014, Rabat, Morocco, [b]University of Zurich, Department of Chemistry, Winterthurerstrasse 190, CH-8057 Zurich, Switzerland, [c]Department of Physics, Hacettepe University, 06800 Beytepe, Ankara, Türkiye, [d]Laboratory of Applied Organic Chemistry, Sidi Mohamed Ben Abdellah University, Faculty of Science And Technology, Road Immouzer, BP 2202 Fez, Morocco, [e]Science and Technology of Lille USR 3290, Villeneuve d'ascq cedex, France, [f]Laboratory of Organic and Physical Chemistry, Applied Bioorganic Chemistry Team, Faculty of Sciences, Ibnou Zohr University, Agadir, Morocco, and [g]Laboratory of Plant Chemistry, Organic and Bioorganic Synthesis, Faculty of Sciences, Mohammed V University in Rabat, 4 Avenue Ibn Battouta BP 1014 RP, Rabat, Morocco. *Correspondence e-mail: mustapha.zouhair@um5r.ac.ma

The benzimidazole entity of the title molecule, $C_{17}H_{21}N_5O$, is almost planar (r.m.s. deviation = 0.0262 Å). In the crystal, bifurcated C—H···O hydrogen bonds link individual molecules into layers extending parallel to the *ac* plane. Two weak C—H···π(ring) interactions may also be effective in the stabilization of the crystal structure. Hirshfeld surface analysis of the crystal structure reveals that the most important contributions for the crystal packing are from H···H (57.9%), H···C/C···H (18.1%) and H···O/O···H (14.9%) interactions. Hydrogen bonding and van der Waals interactions are the most dominant forces in the crystal packing. Evaluation of the electrostatic, dispersion and total energy frameworks indicate that the stabilization of the title compound is dominated *via* dispersion energy contributions. The molecular structure optimized by density functional theory (DFT) at the B3LYP/6–311 G(d,p) level is compared with the experimentally determined molecular structure in the solid state.

1. Chemical context

Heterocyclic compounds comprising the benzimidazolone fragment have attracted interest due to their remarkable usefulness in various therapeutic applications. Extensive research has revealed several pharmacological and biological properties associated with these compounds, including anti-proliferative (Guillon *et al.*, 2022), antibacterial (Al-Ghulikah *et al.*, 2023; Saber *et al.*, 2020), anticancer (Dimov *et al.*, 2021) and antiviral (Ferro *et al.*, 2017) activities.

Our current studies focus on the syntheses of new benzimidazol-2-one derivatives by combining them with the 1,2,3-triazole moiety by using 'click chemistry'. Specifically, the copper-catalysed azide-alkyne cycloaddition (CuAAC) method has proved useful in obtaining the title compound, 1-[(1-butyl-1*H*-1,2,3-triazol-4-yl)methyl]-3-(prop-1-en-2-yl)-1*H*-benzimidazol-2-one (Fig. 1). In this context, we determined its crystal structure, performed a Hirshfeld surface analysis and calculated intermolecular interaction energies

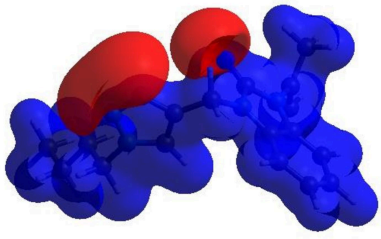

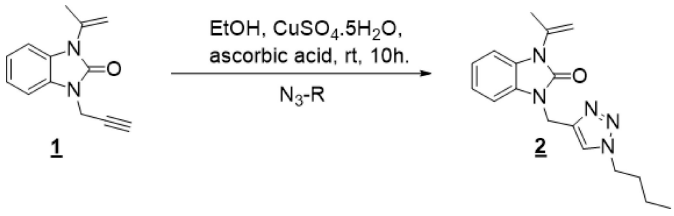

Figure 1
Schematic synthesis procedure for obtaining benzimidazol-2-one derivatives.

and energy frameworks. A comparison of the experimentally determined molecular structure in the solid state with the molecular structure optimized by using density functional theory (DFT) at the B3LYP/6-311G(d,p) level was also carried out.

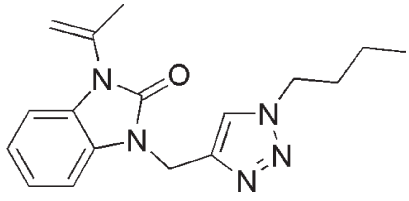

2. Structural commentary

In the molecular structure of the title compound (Fig. 2), the benzimidazole entity is almost planar (r.m.s. deviation of atoms C1–C7/N1–N2/O1 is 0.0262 Å); rings *A* (C1–C6) and *B* (N1/N2/C1/C2/C7) are oriented at a dihedral angle of 1.20 (4)°. The triazole ring *C* (N3–N5/C12/C13) is oriented almost perpendicular to the benzimidazole fragment with dihedral angles of *A*/*C* = 85.36 (4)° and *B*/*C* = 86.52 (4)°. Atoms O1, C8 and C11 are −0.0139 (9) Å, 0.0759 (12) Å and −0.0632 (12) Å away, while atoms C11 and C14 are 0.0245 (11) Å and −0.0835 (13) Å away from the best least-squares planes of rings *B* and *C*, respectively. Hence, they appear almost coplanar with the corresponding ring planes.

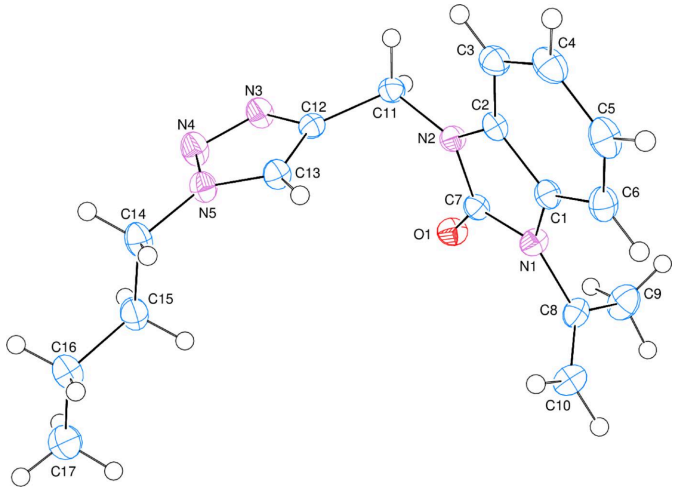

Figure 2
The title molecule with the atom-labelling scheme and displacement ellipsoids drawn at the 50% probability level.

Table 1
Hydrogen-bond geometry (Å, °).

*Cg*1 is the centroid of the C1–C6 ring.

D—H···*A*	*D*—H	H···*A*	*D*···*A*	*D*—H···*A*
C10—H10*B*···O1^{i}	0.987 (17)	2.303 (17)	3.2691 (16)	165.9 (13)
C11—H11*B*···O1^{ii}	0.99	2.35	3.3346 (14)	171
C11—H11*A*···*Cg*1^{i}	0.99	2.70	3.4833 (12)	136
C15—H15*A*···*Cg*1^{iii}	0.99	2.90	3.8400 (13)	159

Symmetry codes: (i) $x-1, y, z$; (ii) $x, -y+\frac{3}{2}, z-\frac{1}{2}$; (iii) $x, -y-\frac{1}{2}, z-\frac{3}{2}$.

3. Supramolecular features

In the crystal, bifurcated C—H···O hydrogen bonds (Table 1, Fig. 3) link individual molecules into layers extending parallel to the *ac* plane. Two weak C—H···π(ring) interactions (Table 1) may also be effective in the stabilization of the crystal packing.

4. Hirshfeld surface analysis

In order to visualize the intermolecular interactions in the crystal structure of the title compound, a Hirshfeld surface (HS) analysis (Hirshfeld, 1977; Spackman & Jayatilaka, 2009) was carried out using *CrystalExplorer* (Spackman *et al.*, 2021). In the HS plotted over d_{norm} (Fig. 4), the white surface indicates contacts with distances equal to the sum of van der Waals radii, and the red and blue surfaces contacts shorter (in close contact) or longer (distinct contact), respectively, than the van

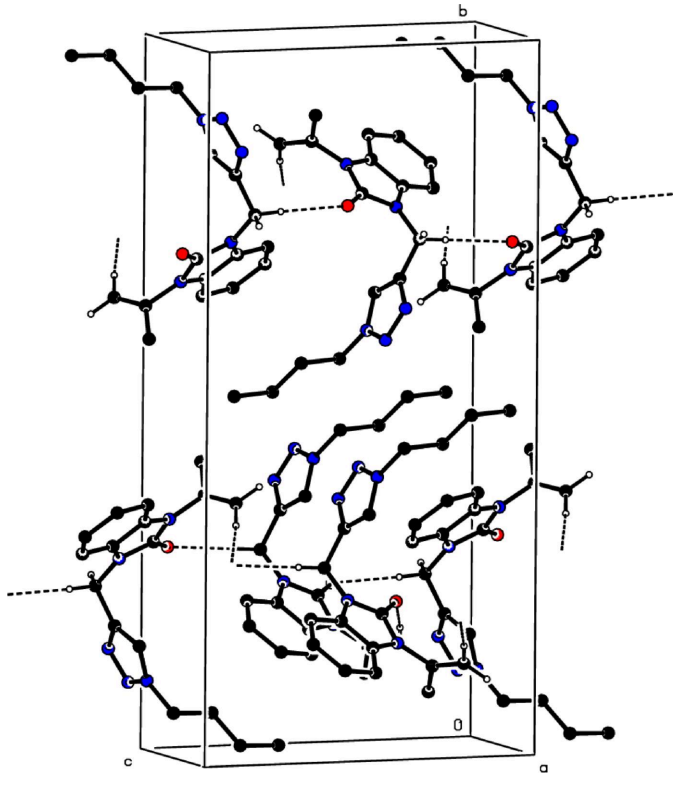

Figure 3
A partial packing diagram of the title compound viewed down the *a* axis. Non-interacting hydrogen atoms were omitted for clarity.

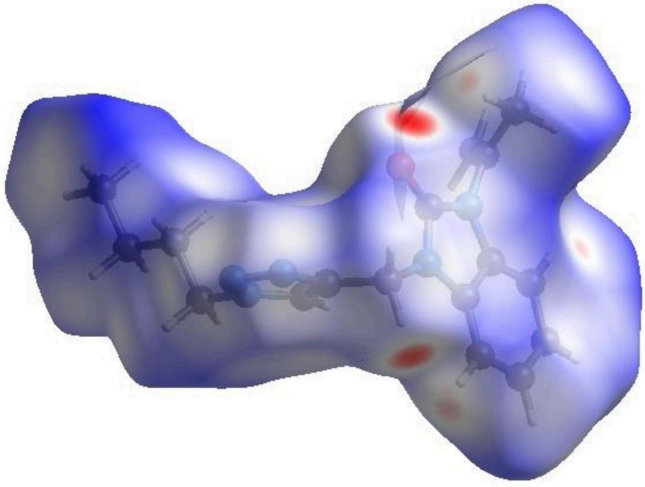

Figure 4
View of the three-dimensional HS of the title compound plotted over d_{norm}.

der Waals radii (Venkatesan *et al.*, 2016). The bright-red spots indicate their roles as the respective donors and/or acceptors; they also appear as blue and red regions corresponding to positive and negative potentials on the HS mapped over electrostatic potential (Spackman *et al.*, 2008; Jayatilaka *et al.*, 2005), as shown in Fig. 5. The blue regions indicate positive electrostatic potential (hydrogen-bond donors), while the red regions indicate negative electrostatic potential (hydrogen-bond acceptors). The shape-index of the HS does not reveal any relevant π–π interactions (Fig. 6). However, the shape-index shows C—H$\cdots\pi$ interactions present as 'red *p*-holes', which are related to the electron ring interactions between the CH groups and the centroids of the aromatic rings of neighbouring molecules (Table 1; Fig. 6). The overall two-dimensional fingerprint plot, Fig. 7*a*, and those delineated into H$\cdots$H, H$\cdots$C/C$\cdots$H, H$\cdots$N/N$\cdots$H, H$\cdots$O/ O$\cdots$H, C$\cdots$N/N$\cdots$C, C$\cdots$C and C$\cdots$O/O$\cdots$C interactions (McKinnon *et al.*, 2007) are illustrated in Fig. 7*b*–*h*, respectively, together with their relative contributions to the HS. The most important interaction is H$\cdots$H contributing with 57.9% to the overall crystal packing, which is reflected in Fig. 7*b* as widely scattered points of high density due to the large hydrogen content of the molecule with the tip at $d_e = d_i = 1.20$ Å. As a result of the presence of C—H$\cdots\pi$ interactions, the H$\cdots$C/C$\cdots$H contacts

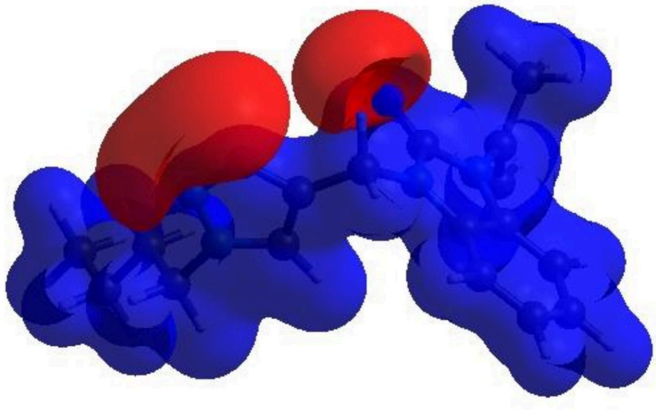

Figure 5
View of the three-dimensional HS of the title compound plotted over electrostatic potential energy using the STO-3 G basis set at the Hartree–Fock level of theory. Hydrogen-bond donors and acceptors are shown as blue and red regions around the atoms corresponding to positive and negative potentials, respectively.

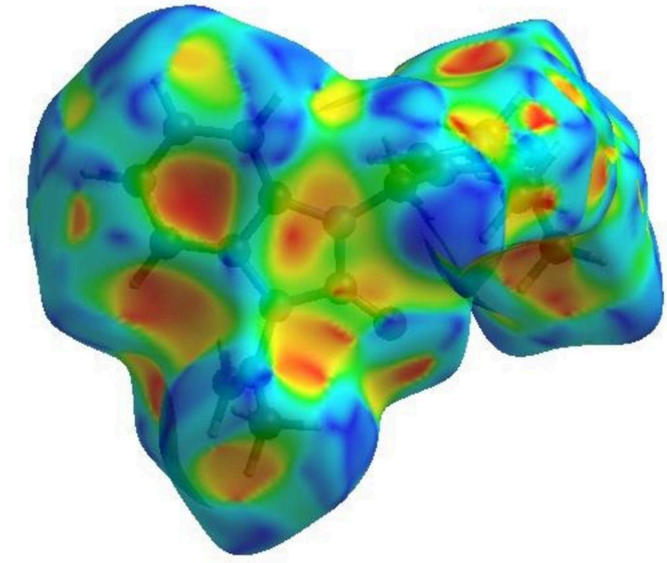

Figure 6
HS of the title compound plotted over shape-index.

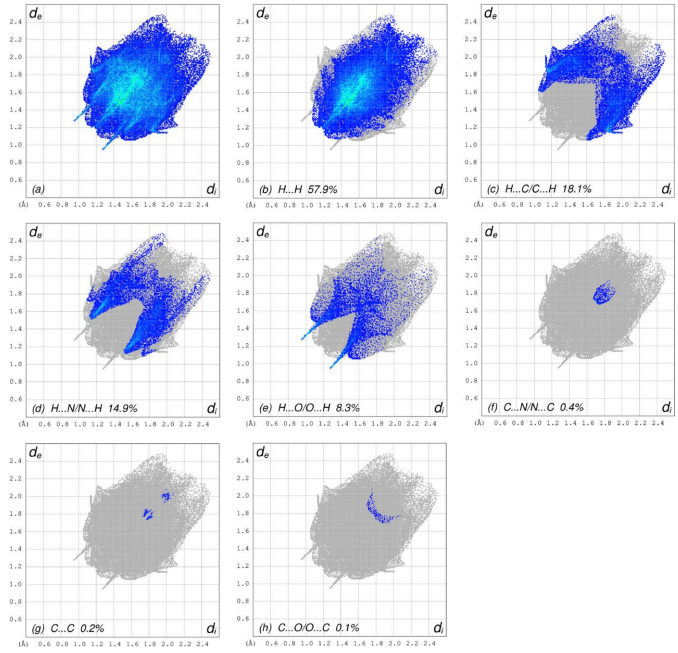

Figure 7
The full two-dimensional fingerprint plots for the title compound, showing (*a*) all interactions, and delineated into (*b*) H$\cdots$H, (*c*) H$\cdots$C/C$\cdots$H, (*d*) H$\cdots$N/N$\cdots$H (*e*) H$\cdots$O/O$\cdots$H, (*f*) C$\cdots$N/N$\cdots$C, (*g*) C$\cdots$C and (*h*) C$\cdots$O/O$\cdots$C interactions. The d_i and d_e values are the closest internal and external distances (in Å) from given points on the Hirshfeld surface.

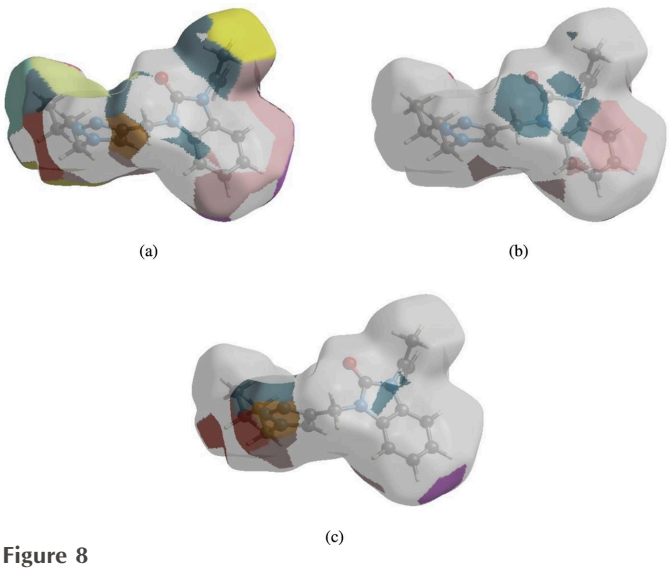

Figure 8
The HS representations with the function d_{norm} plotted onto the surface for (*a*) H···H, (*b*) H···C/C···H and (*c*) H···N/N···H interactions.

contribute 18.1% to the overall crystal packing, as reflected in Fig. 7*c* with the tips at $d_e + d_i = 2.66$ Å. The symmetrical pair of wings in the fingerprint plot delineated into H···N/N···H contacts (Fig. 7*d*), with 14.9% contribution to the HS, has the tips at $d_e + d_i = 2.66$ Å. The symmetrical pair of spikes in the fingerprint plot delineated into H···O/O···H contacts (Fig. 7*e*), 8.3% contribution to the HS, have the tips at $d_e + d_i =$ 2.22 Å. Finally, the C···N/N···C (Fig. 7*f*), C···C (Fig. 7*g*) and C···O/O···C (Fig. 7*h*) interactions make small contibutions of 0.4%, 0.2% and 0.1%, respectively, to the HS.

The nearest neighbour environment of a molecule can be determined from the colour patches on the HS based on how close to other molecules they are. The HS representations with the function d_{norm} plotted onto the surface are shown for the H···H, H···C/C···H and H···N/N···H interactions in Fig. 8*a*–*c*, respectively. The HS analysis confirms the importance of H-atom contacts in establishing the packing. The large number of H···H, H···C/C···H and H···N/N···H interactions suggest that van der Waals and hydrogen-bonding interactions play the major roles in the crystal packing (Hathwar *et al.*, 2015).

5. Interaction energy calculations and energy frameworks

The intermolecular interaction energies were calculated using the CE–B3LYP/6–311G(d,p) energy model available in *CrystalExplorer* (Spackman *et al.*, 2021), where a cluster of molecules is generated by applying crystallographic symmetry operations with respect to a selected central molecule within a radius of 3.8 Å by default (Turner *et al.*, 2014). The total intermolecular energy (E_{tot}) is the sum of electrostatic (E_{ele}), polarization (E_{pol}), dispersion (E_{dis}) and exchange-repulsion (E_{rep}) energies (Turner *et al.*, 2015) with scale factors of 1.057, 0.740, 0.871 and 0.618, respectively (Mackenzie *et al.*, 2017). Hydrogen-bonding interaction energies (in kJ mol^{-1}) were calculated as −32.1 (E_{ele}), −9.4 (E_{pol}), −53.7 (E_{dis}), 48.4 (E_{rep}) and −57.7 (E_{tot}) for C10—H10*B*···O1 and −21.0 (E_{ele}), −7.7 (E_{pol}), −65.2 (E_{dis}), 51.6 (E_{rep}) and −52.8 (E_{tot}) for the C11—H11*B*···O1 hydrogen bond. Energy frameworks combine the calculation of intermolecular interaction energies with a graphical representation of their magnitude (Turner *et al.*, 2015). Energies between molecular pairs are represented as cylinders joining the centroids of pairs of molecules with the cylinder radius proportional to the relative strength of the corresponding interaction energy. Energy frameworks were constructed for E_{ele} (red cylinders), E_{dis} (green cylinders) and E_{tot} (blue cylinders) (Fig. 9*a*–*c*). The evaluation of the electrostatic, dispersion and total energy frameworks indicate that the stabilization is dominated *via* dispersion energies in the crystal structure of the title compound.

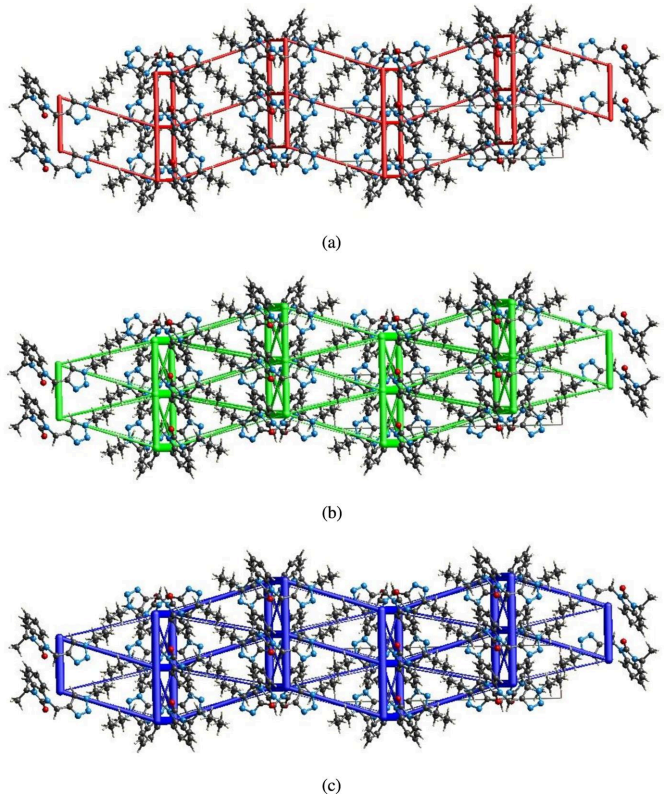

Figure 9
The energy frameworks for a cluster of molecules of the title compound viewed down the *c* axis, showing (*a*) electrostatic energy, (*b*) dispersion energy and (*c*) total energy diagrams. The cylindrical radius is proportional to the relative strength of the corresponding energies and they were adjusted to the same scale factor of 80 with cut-off value of 5 kJ mol^{-1} within 2×2×2 unit cells.

6. DFT calculations

The molecular structure in the gas phase was optimized using density functional theory (DFT) with the B3LYP functional and 6-311G(d,p) basis-set calculations, as implemented in GAUSSIAN 09 (Frisch *et al.* 2009). The optimized parameters, including bond lengths and angles, showed satisfactory agreement with the experimental structural data (Table 2).

Table 2
Comparison of selected (X-ray and DFT) bond length and angles (Å, °).

Bonds/angles	X-ray	B3LYP/6–311G(d,p)
C1—N1	1.3992 (14)	1.352
N1—C7	1.3847 (14)	1.364
N1—C8	1.4402 (14)	1.461
O1—C7	1.2250 (13)	1.235
C2—N2	1.3919 (13)	1.378
N2—C7	1.3770 (14)	1.382
N2—C11	1.4568 (14)	1.438
N3—N4	1.3222 (14)	1.311
N4—N3—C12	108.94 (9)	108.12
N3—N4—N5	106.93 (9)	106.47
N4—N5—C13	111.07 (9)	111.64
N4—N5—C14	120.09 (9)	120.71
C13—N5—C14	128.71 (10)	128.48
N2—C7—N1	106.56 (9)	106.29
N3—N4—N5—C13	0.00 (13)	0.02
N3—C12—C13—N5	–0.12 (12)	0.18
C1—N1—C7—O1	–178.68 (11)	–178.74
C1—N1—C7—N2	0.08 (12)	0.07

The largest differences between the calculated and experimental values were observed for the C1—N1 (0.04 Å), N1—C7 and N1—C8 (0.02 Å) bond lengths, the N4—N3—C12 (0.82°) bond angle and the torsion angle N3—C12—C13—N5 (0.3°). These differences may be due to the fact that the calculations are based on an isolated molecule at 0 K, while the experimental results were obtained from interacting molecules in the solid state, where intra- and intermolecular interactions with neighbouring molecules are present.

7. Database survey

A survey of the Cambridge Structural Database (CSD, updated March 2024; Groom *et al.*, 2016) indicates that there are several molecules similar to the title compound (Fig. 10). These include I (CSD refcode YIVWUZ; Zouhair *et al.*, 2023), II with R_1 = –C_6H_9, R_2 = –C_6H_5 and R_3 = H (CSD refcode PAZFOO; Adardour *et al.*, 2017), III with R_1 = –$C(CH_3)$═CH_2, R_2 = –$C_{10}H_{\mathbf{22}}$ and R_3 = –H (CSD refcode ETAJOB; Saber *et al.*, 2021) and IV with R_1 = –$CH_2C_6H_5$, R_2 = -$C_{12}H_{26}$ and R_3 = H (CSD refcode ETAKAO; Saber *et al.*, 2021). The benzimidazol-2-one unit in all of these compounds is almost planar, with the dihedral angle between the constituent rings being less than 1°, or having the nitrogen atom bearing the exocyclic substituent less than 0.03 Å from the mean plane of the remaining nine atoms.

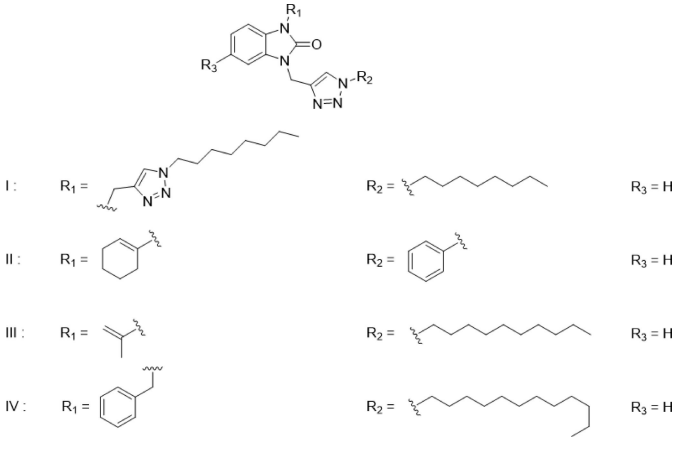

Figure 10
Related molecular fragments for searching the CSD database.

Table 3
Experimental details.

Crystal data	
Chemical formula	$C_{17}H_{21}N_5O$
M_r	311.39
Crystal system, space group	Monoclinic, $P2_1/c$
Temperature (K)	160
a, b, c (Å)	5.7032 (1), 24.2184 (5), 11.8683 (2)
β (°)	91.312 (2)
V (Å^3)	1638.85 (5)
Z	4
Radiation type	Cu $K\alpha$
μ (mm^{-1})	0.66
Crystal size (mm)	0.19 × 0.12 × 0.05
Data collection	
Diffractometer	SuperNova, Dual, Cu at home/near, Atlas
Absorption correction	Analytical [*CrysAlis PRO* (Rigaku OD, 2023) using a multifaceted crystal model (Clark & Reid, 1995)]
T_{min}, T_{max}	0.894, 0.971
No. of measured, independent and observed [$I > 2\sigma(I)$] reflections	19825, 3435, 2968
R_{int}	0.034
(sin $\theta/\lambda)_{max}$ (Å^{-1})	0.631
Refinement	
$R[F^2 > 2\sigma(F^2)]$, $wR(F^2)$, S	0.034, 0.086, 1.05
No. of reflections	3435
No. of parameters	219
H-atom treatment	H atoms treated by a mixture of independent and constrained refinement
$\Delta\rho_{max}$, $\Delta\rho_{min}$ (e Å^{-3})	0.22, −0.21

Computer programs: *CrysAlis PRO* (Rigaku OD, 2023), *SHELXT* (Sheldrick, 2015*a*), *SHELXL* (Sheldrick, 2015*b*), *OLEX2* (Dolomanov *et al.*, 2009) and *publCIF* (Westrip, 2010).

8. Synthesis and crystallization

To a solution of 2.87 mmol of 1-(prop-1-en-2-yl)-3-(prop-2-ynyl)-1*H*-benzimidazol-2-one and 0.45 mmol of 1-azidobutane in 10 ml of ethanol were added 1.64 mmol of $CuSO_4$ and 3.73 mmol of sodium ascorbate dissolved in 10 ml of distilled water. The reaction mixture was stirred for 10 h at room temperature and monitored by TLC. After filtration and concentration of the solution under reduced pressure, the residue obtained was chromatographed on a silica gel column using ethyl acetate/hexane (3/1) as eluent. The resulting solid was filtered off, washed with water, dried, and then recrystallized from ethanol, yield: 73%.

9. Refinement

Crystal data, data collection and structure refinement details are summarized in Table 3. Methylene hydrogens attached to

C10 were located in a difference-Fourier map, and were included as riding contributions in idealized positions with $U_{iso}(H) = 1.2U_{eq}(C)$. Aromatic H atoms were treated the same way, and methyl H atoms with $U_{iso}(H) = 1.5U_{eq}(C)$.

Funding information

TH is grateful to Hacettepe University Scientific Research Project Unit (grant No. 013 D04 602 004).

References

Adardour, M., Loughzail, M., Dahaoui, S., Baouid, A. & Berraho, M. (2017). *IUCrData*, **2**, x170907.
Al-Ghulikah, H., Ghabi, A., haouas, A., Mtiraoui, H., Jeanneau, E. & Msaddek, M. (2023). *Arab. J. Chem.* **16**, 104566.
Clark, R. C. & Reid, J. S. (1995). *Acta Cryst.* A**51**, 887–897.
Dimov, S., Mavrova, A. T., Yancheva, D., Nikolova, B. & Tsoneva, I. (2021). *Anticancer Agents Med. Chem.* **21**, 1441–1450.
Dolomanov, O. V., Bourhis, L. J., Gildea, R. J., Howard, J. A. K. & Puschmann, H. (2009). *J. Appl. Cryst.* **42**, 339–341.
Ferro, S., Buemi, M. R., De Luca, L., Agharbaoui, F. E., Pannecouque, C. & Monforte, A. M. (2017). *Bioorg. & Med. Chem.* **25**, 3861–3870.
Frisch, M. J., Trucks, G. W., Schlegel, H. B., Scuseria, G. E., Robb, M. A., Cheeseman, J. R., Scalmani, G., Barone, V., Mennucci, B., Petersson, G. A., Nakatsuji, H., Caricato, M., Li, X., Hratchian, H. P., Izmaylov, A. F., Bloino, J., Zheng, G., Sonnenberg, J. L., Hada, M., Ehara, M., Toyota, K., Fukuda, R., Hasegawa, J., Ishida, M., Nakajima, T., Honda, Y., Kitao, O., Nakai, H., Vreven, T., Montgomery, J. A. Jr, Peralta, J. E., Ogliaro, F., Bearpark, M., Heyd, J. J., Brothers, E., Kudin, K. N., Staroverov, V. N., Kobayashi, R., Normand, J., Raghavachari, K., Rendell, A., Burant, J. C., Iyengar, S. S., Tomasi, J., Cossi, M., Rega, N., Millam, J. M., Klene, M., Knox, J. E., Cross, J. B., Bakken, V., Adamo, C., Jaramillo, J., Gomperts, R., Stratmann, R. E., Yazyev, O., Austin, A. J., Cammi, R., Pomelli, C., Ochterski, J. W., Martin, R. L., Morokuma, K., Zakrzewski, V. G., Voth, G. A., Salvador, P., Dannenberg, J. J., Dapprich, S., Daniels, A. D., Farkas, O., Foresman, J. B., Ortiz, J. V., Cioslowski, J. & Fox, D. J. (2009). *GAUSSIAN09*. Gaussian Inc., Wallingford, CT, USA.
Groom, C. R., Bruno, I. J., Lightfoot, M. P. & Ward, S. C. (2016). *Acta Cryst.* B**72**, 171–179.
Guillon, J., Savrimoutou, S., Albenque-Rubio, S., Pinaud, N., Moreau, S. & Desplat, V. (2022). *Molbank*, M1333.
Hathwar, V. R., Sist, M., Jørgensen, M. R. V., Mamakhel, A. H., Wang, X., Hoffmann, C. M., Sugimoto, K., Overgaard, J. & Iversen, B. B. (2015). *IUCrJ*, **2**, 563–574.
Hirshfeld, H. L. (1977). *Theor. Chim. Acta*, **44**, 129–138.
Jayatilaka, D., Grimwood, D. J., Lee, A., Lemay, A., Russel, A. J., Taylor, C., Wolff, S. K., Cassam-Chenai, P. & Whitton, A. (2005). *TONTO* – A System for Computational Chemistry. Available at: http://hirshfeldsurface.net/
Mackenzie, C. F., Spackman, P. R., Jayatilaka, D. & Spackman, M. A. (2017). *IUCrJ*, **4**, 575–587.
McKinnon, J. J., Jayatilaka, D. & Spackman, M. A. (2007). *Chem. Commun.* pp. 3814–3816.
Rigaku, OD (2023). *CrysAlis PRO*. Rigaku Oxford Diffraction, Yarnton, England..
Saber, A., Anouar, E. H., Sebbar, G., Ibrahimi, B. E., Srhir, M., Hökelek, T., Mague, J. T., Ghayati, L. E., Sebbar, N. K. & Essassi, E. M. (2021). *J. Mol. Struct.* **1242**, 130719.
Saber, A., Sebbar, N. K., Sert, Y., Alzaqri, N., Hökelek, T., El Ghayati, L., Talbaoui, A., Mague, J. T., Baba, Y., Urrutigoîty, M. & Essassi, E. M. (2020). *J. Mol. Struct.* **1200**, 127174.
Sheldrick, G. M. (2015*a*). *Acta Cryst.* A**71**, 3–8.
Sheldrick, G. M. (2015*b*). *Acta Cryst.* C**71**, 3–8.
Spackman, M. A. & Jayatilaka, D. (2009). *CrystEngComm*, **11**, 19–32.
Spackman, M. A., McKinnon, J. J. & Jayatilaka, D. (2008). *CrystEngComm*, **10**, 377–388.
Spackman, P. R., Turner, M. J., McKinnon, J. J., Wolff, S. K., Grimwood, D. J., Jayatilaka, D. & Spackman, M. A. (2021). *J. Appl. Cryst.* **54**, 1006–1011.
Turner, M. J., Grabowsky, S., Jayatilaka, D. & Spackman, M. A. (2014). *J. Phys. Chem. Lett.* **5**, 4249–4255.
Turner, M. J., Thomas, S. P., Shi, M. W., Jayatilaka, D. & Spackman, M. A. (2015). *Chem. Commun.* **51**, 3735–3738.
Venkatesan, P., Thamotharan, S., Ilangovan, A., Liang, H. & Sundius, T. (2016). *Spectrochim. Acta A Mol. Biomol. Spectrosc.* **153**, 625–636.
Westrip, S. P. (2010). *J. Appl. Cryst.* **43**, 920–925.
Zouhair, M., El Ghayati, L., El Monfalouti, H., Abchihi, H., Hökelek, T., Ahmed, M., Mague, J. T. & Sebbar, N. K. (2023). *Acta Cryst.* E**79**, 1179–1182.

supporting information

Acta Cryst. (2024). E**80**, 601-606 [https://doi.org/10.1107/S2056989024004043]

Crystal structure, Hirshfeld surface analysis, calculations of intermolecular interaction energies and energy frameworks and the DFT-optimized molecular structure of 1-[(1-butyl-1*H*-1,2,3-triazol-4-yl)methyl]-3-(prop-1-en-2-yl)-1*H*-benzimidazol-2-one

Zakaria El Atrassi, Mustapha Zouhair, Olivier Blacque, Tuncer Hökelek, Amal Haoudi, Ahmed Mazzah, Hassan Cherkaoui and Nada Kheira Sebbar

Computing details

1-[(1-Butyl-1*H*-1,2,3-triazol-4-yl)methyl]-3-(prop-1-en-2-yl)-1*H*-benzimidazol-2-one

Crystal data

$C_{17}H_{21}N_5O$
$M_r = 311.39$
Monoclinic, $P2_1/c$
$a = 5.7032$ (1) Å
$b = 24.2184$ (5) Å
$c = 11.8683$ (2) Å
$\beta = 91.312$ (2)°
$V = 1638.85$ (5) Å^3
$Z = 4$
$F(000) = 664$
$D_x = 1.262$ Mg m^{-3}
Cu $K\alpha$ radiation, $\lambda = 1.54184$ Å
Cell parameters from 10273 reflections
$\theta = 3.6$–$76.4°$
$\mu = 0.66$ mm^{-1}
$T = 160$ K
Plate, colourless
0.19 × 0.12 × 0.05 mm

Data collection

SuperNova, Dual, Cu at home/near, Atlas diffractometer
Radiation source: micro-focus sealed X-ray tube, SuperNova (Cu) X-ray Source
Mirror monochromator
Detector resolution: 10.3801 pixels mm^{-1}
ω scans
Absorption correction: analytical [CrysAlisPro (Rigaku OD, 2023) using a multifaceted crystal model (Clark & Reid, 1995)]
$T_{min} = 0.894$, $T_{max} = 0.971$
19825 measured reflections
3435 independent reflections
2968 reflections with $I > 2\sigma(I)$
$R_{int} = 0.034$
$\theta_{max} = 76.8°$, $\theta_{min} = 3.7°$
$h = -7\rightarrow7$
$k = -30\rightarrow26$
$l = -14\rightarrow14$

Refinement

Refinement on F^2
Least-squares matrix: full
$R[F^2 > 2\sigma(F^2)] = 0.034$
$wR(F^2) = 0.086$
$S = 1.05$
3435 reflections
219 parameters
0 restraints
Primary atom site location: dual
Hydrogen site location: mixed

H atoms treated by a mixture of independent and constrained refinement
$w = 1/[\sigma^2(F_o^2) + (0.0353P)^2 + 0.4935P]$ where $P = (F_o^2 + 2F_c^2)/3$
$(\Delta/\sigma)_{max} = 0.001$
$\Delta\rho_{max} = 0.22$ e Å^{-3}
$\Delta\rho_{min} = -0.21$ e Å^{-3}
Extinction correction: SHELXL (Sheldrick, 2015b), $Fc^* = kFc[1+0.001xFc^2\lambda^3/\sin(2\theta)]^{-1/4}$
Extinction coefficient: 0.0018 (2)

Special details

Geometry. All esds (except the esd in the dihedral angle between two l.s. planes) are estimated using the full covariance matrix. The cell esds are taken into account individually in the estimation of esds in distances, angles and torsion angles; correlations between esds in cell parameters are only used when they are defined by crystal symmetry. An approximate (isotropic) treatment of cell esds is used for estimating esds involving l.s. planes.

Fractional atomic coordinates and isotropic or equivalent isotropic displacement parameters (Å²)

	x	*y*	*z*	U_{iso}*/U_{eq}
C1	0.57633 (19)	0.82949 (4)	0.42568 (9)	0.0208 (2)
N1	0.71001 (16)	0.82797 (4)	0.52597 (8)	0.0223 (2)
O1	1.04428 (14)	0.77946 (4)	0.58607 (6)	0.02597 (19)
C2	0.68397 (19)	0.79364 (4)	0.35005 (9)	0.0202 (2)
N2	0.87645 (16)	0.77053 (4)	0.40675 (7)	0.0203 (2)
N3	1.17211 (17)	0.63652 (4)	0.43348 (9)	0.0262 (2)
C3	0.5972 (2)	0.78704 (5)	0.24096 (9)	0.0252 (2)
H3	0.671876	0.763257	0.189186	0.030*
C4	0.3964 (2)	0.81658 (5)	0.21003 (10)	0.0298 (3)
H4	0.332148	0.812748	0.135891	0.036*
N4	1.08726 (18)	0.59076 (4)	0.47758 (9)	0.0300 (2)
C5	0.2882 (2)	0.85168 (5)	0.28603 (11)	0.0302 (3)
H5	0.151175	0.871223	0.262565	0.036*
N5	0.85618 (17)	0.59867 (4)	0.48951 (8)	0.0245 (2)
C6	0.3761 (2)	0.85880 (5)	0.39558 (10)	0.0264 (2)
H6	0.301892	0.882696	0.447298	0.032*
C7	0.89510 (19)	0.79157 (5)	0.51438 (9)	0.0206 (2)
H10A	0.459 (3)	0.8759 (7)	0.7493 (13)	0.037 (4)*
H10B	0.365 (3)	0.8256 (7)	0.6610 (13)	0.041 (4)*
C8	0.6746 (2)	0.86076 (5)	0.62539 (9)	0.0235 (2)
C9	0.8628 (2)	0.90232 (6)	0.65046 (12)	0.0349 (3)
H9A	1.013615	0.883371	0.660827	0.052*
H9B	0.825804	0.922450	0.719442	0.052*
H9C	0.872346	0.928362	0.587528	0.052*
C10	0.4838 (2)	0.85325 (5)	0.68373 (11)	0.0296 (3)
C11	1.03801 (19)	0.72874 (5)	0.36645 (9)	0.0221 (2)
H11A	1.200895	0.740317	0.384875	0.027*
H11B	1.021480	0.725930	0.283427	0.027*
C12	0.99452 (19)	0.67315 (5)	0.41755 (9)	0.0201 (2)
C13	0.79133 (19)	0.64923 (5)	0.45341 (9)	0.0230 (2)
H13	0.638578	0.664893	0.452876	0.028*
C14	0.7134 (2)	0.55616 (5)	0.54332 (11)	0.0289 (3)
H14A	0.746715	0.519827	0.508967	0.035*
H14B	0.545234	0.564507	0.529705	0.035*

C15	0.7638 (2)	0.55325 (5)	0.66936 (11)	0.0297 (3)
H15A	0.733683	0.589859	0.703238	0.036*
H15B	0.931469	0.544300	0.682716	0.036*
C16	0.6139 (3)	0.51012 (6)	0.72697 (12)	0.0392 (3)
H16A	0.446195	0.519093	0.713803	0.047*
H16B	0.643818	0.473503	0.693086	0.047*
C17	0.6652 (3)	0.50730 (6)	0.85305 (13)	0.0462 (4)
H17A	0.832201	0.499571	0.866492	0.069*
H17B	0.571337	0.477838	0.886196	0.069*
H17C	0.625225	0.542686	0.887757	0.069*

Atomic displacement parameters (Å²)

	U^{11}	U^{22}	U^{33}	U^{12}	U^{13}	U^{23}
C1	0.0202 (5)	0.0196 (5)	0.0226 (5)	−0.0020 (4)	−0.0017 (4)	0.0017 (4)
N1	0.0207 (4)	0.0248 (5)	0.0214 (5)	0.0030 (4)	−0.0015 (3)	−0.0022 (4)
O1	0.0235 (4)	0.0322 (4)	0.0221 (4)	0.0034 (3)	−0.0036 (3)	0.0013 (3)
C2	0.0193 (5)	0.0188 (5)	0.0223 (5)	−0.0020 (4)	−0.0008 (4)	0.0037 (4)
N2	0.0203 (4)	0.0214 (5)	0.0193 (4)	0.0022 (4)	−0.0003 (3)	0.0006 (3)
N3	0.0205 (5)	0.0255 (5)	0.0329 (5)	0.0027 (4)	0.0022 (4)	0.0050 (4)
C3	0.0283 (6)	0.0252 (6)	0.0220 (5)	−0.0036 (5)	−0.0017 (4)	0.0010 (4)
C4	0.0309 (6)	0.0318 (6)	0.0262 (6)	−0.0047 (5)	−0.0081 (5)	0.0067 (5)
N4	0.0223 (5)	0.0254 (5)	0.0424 (6)	0.0038 (4)	0.0038 (4)	0.0068 (4)
C5	0.0233 (6)	0.0291 (6)	0.0379 (7)	0.0002 (5)	−0.0072 (5)	0.0086 (5)
N5	0.0203 (5)	0.0228 (5)	0.0302 (5)	−0.0011 (4)	0.0002 (4)	0.0026 (4)
C6	0.0224 (5)	0.0235 (6)	0.0332 (6)	0.0016 (4)	−0.0008 (4)	0.0028 (5)
C7	0.0195 (5)	0.0215 (5)	0.0210 (5)	−0.0009 (4)	0.0010 (4)	0.0019 (4)
C8	0.0248 (5)	0.0214 (5)	0.0241 (5)	0.0025 (4)	−0.0027 (4)	−0.0035 (4)
C9	0.0308 (6)	0.0317 (7)	0.0422 (7)	−0.0055 (5)	−0.0005 (5)	−0.0098 (5)
C10	0.0275 (6)	0.0325 (6)	0.0290 (6)	0.0029 (5)	0.0018 (5)	−0.0057 (5)
C11	0.0221 (5)	0.0224 (5)	0.0219 (5)	0.0022 (4)	0.0042 (4)	0.0016 (4)
C12	0.0198 (5)	0.0220 (5)	0.0186 (5)	0.0017 (4)	−0.0012 (4)	−0.0008 (4)
C13	0.0189 (5)	0.0234 (5)	0.0268 (5)	0.0019 (4)	−0.0007 (4)	0.0022 (4)
C14	0.0259 (6)	0.0237 (6)	0.0372 (7)	−0.0056 (5)	0.0001 (5)	0.0038 (5)
C15	0.0291 (6)	0.0242 (6)	0.0358 (7)	−0.0014 (5)	0.0025 (5)	0.0029 (5)
C16	0.0488 (8)	0.0292 (7)	0.0401 (7)	−0.0074 (6)	0.0097 (6)	0.0037 (5)
C17	0.0656 (10)	0.0335 (7)	0.0399 (8)	0.0074 (7)	0.0122 (7)	0.0062 (6)

Geometric parameters (Å, º)

C1—N1	1.3992 (14)	C8—C10	1.3158 (17)
C1—C2	1.4007 (15)	C9—H9A	0.9800
C1—C6	1.3847 (16)	C9—H9B	0.9800
N1—C7	1.3847 (14)	C9—H9C	0.9800
N1—C8	1.4402 (14)	C10—H10A	0.966 (16)
O1—C7	1.2250 (13)	C10—H10B	0.987 (17)
C2—N2	1.3919 (13)	C11—H11A	0.9900
C2—C3	1.3846 (16)	C11—H11B	0.9900

N2—C7	1.3770 (14)	C11—C12	1.4995 (15)
N2—C11	1.4568 (14)	C12—C13	1.3719 (15)
N3—N4	1.3222 (14)	C13—H13	0.9500
N3—C12	1.3564 (14)	C14—H14A	0.9900
C3—H3	0.9500	C14—H14B	0.9900
C3—C4	1.3924 (17)	C14—C15	1.5184 (17)
C4—H4	0.9500	C15—H15A	0.9900
C4—C5	1.3938 (19)	C15—H15B	0.9900
N4—N5	1.3424 (13)	C15—C16	1.5218 (17)
C5—H5	0.9500	C16—H16A	0.9900
C5—C6	1.3933 (17)	C16—H16B	0.9900
N5—C13	1.3464 (15)	C16—C17	1.520 (2)
N5—C14	1.4678 (15)	C17—H17A	0.9800
C6—H6	0.9500	C17—H17B	0.9800
C8—C9	1.4965 (16)	C17—H17C	0.9800

N1—C1—C2	106.90 (9)	H9B—C9—H9C	109.5
C6—C1—N1	131.54 (11)	H10A—C10—H10B	119.5 (13)
C6—C1—C2	121.57 (10)	C8—C10—H10A	119.0 (9)
C1—N1—C8	126.77 (9)	C8—C10—H10B	121.5 (9)
C7—N1—C1	109.51 (9)	N2—C11—H11A	109.1
C7—N1—C8	123.64 (9)	N2—C11—H11B	109.1
N2—C2—C1	106.96 (9)	N2—C11—C12	112.28 (9)
C3—C2—C1	121.22 (10)	H11A—C11—H11B	107.9
C3—C2—N2	131.81 (11)	C12—C11—H11A	109.1
C2—N2—C11	128.19 (9)	C12—C11—H11B	109.1
C7—N2—C2	110.06 (9)	N3—C12—C11	120.90 (10)
C7—N2—C11	121.71 (9)	N3—C12—C13	108.30 (10)
N4—N3—C12	108.94 (9)	C13—C12—C11	130.79 (10)
C2—C3—H3	121.3	N5—C13—C12	104.77 (10)
C2—C3—C4	117.47 (11)	N5—C13—H13	127.6
C4—C3—H3	121.3	C12—C13—H13	127.6
C3—C4—H4	119.5	N5—C14—H14A	109.3
C3—C4—C5	121.10 (11)	N5—C14—H14B	109.3
C5—C4—H4	119.5	N5—C14—C15	111.53 (10)
N3—N4—N5	106.93 (9)	H14A—C14—H14B	108.0
C4—C5—H5	119.2	C15—C14—H14A	109.3
C6—C5—C4	121.62 (11)	C15—C14—H14B	109.3
C6—C5—H5	119.2	C14—C15—H15A	109.1
N4—N5—C13	111.07 (9)	C14—C15—H15B	109.1
N4—N5—C14	120.09 (9)	C14—C15—C16	112.28 (11)
C13—N5—C14	128.71 (10)	H15A—C15—H15B	107.9
C1—C6—C5	117.01 (11)	C16—C15—H15A	109.1
C1—C6—H6	121.5	C16—C15—H15B	109.1
C5—C6—H6	121.5	C15—C16—H16A	109.2
O1—C7—N1	127.03 (10)	C15—C16—H16B	109.2
O1—C7—N2	126.40 (10)	H16A—C16—H16B	107.9
N2—C7—N1	106.56 (9)	C17—C16—C15	112.07 (12)

N1—C8—C9	114.85 (10)	C17—C16—H16A	109.2
C10—C8—N1	119.21 (11)	C17—C16—H16B	109.2
C10—C8—C9	125.91 (11)	C16—C17—H17A	109.5
C8—C9—H9A	109.5	C16—C17—H17B	109.5
C8—C9—H9B	109.5	C16—C17—H17C	109.5
C8—C9—H9C	109.5	H17A—C17—H17B	109.5
H9A—C9—H9B	109.5	H17A—C17—H17C	109.5
H9A—C9—H9C	109.5	H17B—C17—H17C	109.5
C1—N1—C7—O1	−178.68 (11)	C3—C2—N2—C11	−4.13 (19)
C1—N1—C7—N2	0.08 (12)	C3—C4—C5—C6	0.16 (19)
C1—N1—C8—C9	−112.17 (13)	C4—C5—C6—C1	0.11 (18)
C1—N1—C8—C10	66.21 (16)	N4—N3—C12—C11	−178.92 (10)
C1—C2—N2—C7	−1.17 (12)	N4—N3—C12—C13	0.13 (13)
C1—C2—N2—C11	176.71 (10)	N4—N5—C13—C12	0.08 (13)
C1—C2—C3—C4	−1.20 (17)	N4—N5—C14—C15	71.86 (14)
N1—C1—C2—N2	1.18 (12)	N5—C14—C15—C16	178.92 (11)
N1—C1—C2—C3	−178.09 (10)	C6—C1—N1—C7	179.65 (12)
N1—C1—C6—C5	178.57 (12)	C6—C1—N1—C8	−3.6 (2)
C2—C1—N1—C7	−0.79 (12)	C6—C1—C2—N2	−179.20 (10)
C2—C1—N1—C8	175.93 (10)	C6—C1—C2—C3	1.53 (17)
C2—C1—C6—C5	−0.93 (17)	C7—N1—C8—C9	64.12 (15)
C2—N2—C7—N1	0.68 (12)	C7—N1—C8—C10	−117.50 (13)
C2—N2—C7—O1	179.46 (11)	C7—N2—C11—C12	72.83 (13)
C2—N2—C11—C12	−104.83 (12)	C8—N1—C7—O1	4.47 (18)
C2—C3—C4—C5	0.38 (18)	C8—N1—C7—N2	−176.77 (10)
N2—C2—C3—C4	179.74 (11)	C11—N2—C7—N1	−177.36 (9)
N2—C11—C12—N3	−150.31 (10)	C11—N2—C7—O1	1.41 (17)
N2—C11—C12—C13	30.88 (16)	C11—C12—C13—N5	178.80 (11)
N3—N4—N5—C13	0.00 (13)	C12—N3—N4—N5	−0.08 (13)
N3—N4—N5—C14	−176.20 (10)	C13—N5—C14—C15	−103.59 (14)
N3—C12—C13—N5	−0.12 (12)	C14—N5—C13—C12	175.86 (11)
C3—C2—N2—C7	177.99 (12)	C14—C15—C16—C17	179.91 (12)

Hydrogen-bond geometry (Å, º)

*Cg*1 is the centroid of the C1–C6 ring.

D—H···*A*	*D*—H	H···*A*	*D*···*A*	*D*—H···*A*
C10—H10*B*···O1^{i}	0.987 (17)	2.303 (17)	3.2691 (16)	165.9 (13)
C11—H11*B*···O1^{ii}	0.99	2.35	3.3346 (14)	171
C11—H11*A*···*Cg*1^{i}	0.99	2.70	3.4833 (12)	136
C15—H15*A*···*Cg*1^{iii}	0.99	2.90	3.8400 (13)	159

Symmetry codes: (i) *x*−1, *y*, *z*; (ii) *x*, −*y*+3/2, *z*−1/2; (iii) *x*, −*y*−1/2, *z*−3/2.